Mon. Not. R. Astron. Soc. **358,** 1215–1230 (2005) doi:10.1111/j.1365-2966.2005.08694.x

Tracing the formation history of intermediate-age star clusters in the Small Magellanic Cloud

Andrés E. Piatti,[1★] Ata Sarajedini,[2★] Doug Geisler,[3★] Juan Seguel[3,4★] and David Clark[2★]

[1]*Instituto de Astronomía y Física del Espacio, CC 67, Suc. 28, 1428, Ciudad de Buenos Aires, Argentina*
[2]*Department of Astronomy, University of Florida, PO Box 112055, Gainesville, FL 32611, USA*
[3]*Grupo de Astronomía, Departamento de Física, Universidad de Concepción, Casilla 160-C, Concepción, Chile*
[4]*Cerro Tololo Inter-American Observatory, Casilla 603, La Serena, Chile*

Accepted 2005 February 4. Received 2005 February 4; in original form 2004 November 5

ABSTRACT

Colour–magnitude diagrams (CMDs) are presented for the first time for 10 star clusters projected on to the Small Magellanic Cloud (SMC). The photometry was carried out in the Washington system C and T_1 filters allowing the determination of ages by means of the magnitude difference between the red giant clump and the main-sequence turnoff (MSTO), and metallicities from the red giant branch (RGB) locus. The clusters all have ages in the range 1.5–4 Gyr and metallicities between $-1.3 <$ [Fe/H] < -0.6, with respective errors of $\sim$0.5 Gyr and 0.3 dex. This increases substantially the sample of intermediate-age clusters in the SMC with well-derived parameters. We combine our results with those for other clusters in the literature to derive as large and homogeneous a data base as possible (totalling 26 clusters) in order to study global effects. We find evidence for two peaks in the age distribution of SMC clusters, at $\sim$6.5 and 2.5 Gyr, in good agreement with previous hints involving smaller samples. The most recent peak occurs at a time that corresponds to a very close encounter between the Large Magellanic Cloud (LMC) and the SMC according to the recent dynamical models of Bekki et al. that they used to explain the enhancement of LMC clusters with this age. It appears cluster formation may have been similarly stimulated in the SMC by this encounter as well. We also find very good agreement between cluster ages and metallicities and the prediction from a bursting model from Pagel and Tautvaišienė with a burst that occurred 3 Gyr ago. These two lines of evidence together favour a bursting cluster formation history as opposed to a continuous one for the SMC.

Key words: techniques: photometric – galaxies: individual: SMC – Magellanic Clouds – galaxies: star clusters.

1 INTRODUCTION

Although the Small Magellanic Cloud (SMC) has a large number of relatively bright star clusters, suprisingly few have been studied in much detail. Indeed, Piatti et al. (2001) listed a total of only 16 clusters with ages and metallicities placed on to a homogeneous scale. From these, they investigated the SMC cluster age–metallicity relationship (AMR) and found that the chemical enrichment was not very efficient up until approximately 5 Gyr ago. Over the next several Gyrs, the mean metallicity increased on average from [Fe/H] ~ -1.5 up to -1.1 dex (see their fig. 11). Over the last $\sim$3 Gyr, the metallicity has increased at a similar rate, to a present-day value of ~ -0.6.

The SMC AMR has received greater attention from the theoretical standpoint. Stryker, Da Costa & Mould (1985), Da Costa (1991) and Olszewski, Suntzeff & Mateo (1996), among others, argued that the AMR has fundamentally two components. First, a presumed initial burst of star formation brought the cluster abundances up to [Fe/H] ≈ -1.3; the subsequent net rate of enrichment being very low until perhaps 2–3 Gyr ago. Secondly, at about this same time, the rate of enrichment apparently increased and brought the cluster abundances up to the present-day value. This sort of AMR is very different from that expected from the simple model of chemical evolution. However, for Da Costa & Hatzidimitriou (1998), the enrichment history of the SMC indicated in their fig. 4 suggests a

★E-mail: andres@iafe.uba.ar (AEP); ata@astro.ufl.edu (AS); doug@kukita.cfm.udec.cl (DG); jseguel@andromeda.cfm.udec.cl (JS); dmclark@polaris.astro.ufl.edu (DC)

Table 1. Observations log of selected clusters.

Star cluster[a]	α_{2000} (h m s)	δ_{2000} (° ′ ″)	l (°)	b (°)	Date	Filter	Exposure (s)	Airmass	Seeing (arcsec)
L 4=K 1, ESO 28-SC15	0 21 27	−73 44 55	305.80	−43.21	2002 Oct 31	*C*	2400	1.40	1.7
						R	800	1.38	1.5
					2003 Dec 02	*C*	180	1.42	1.3
						R	60	1.43	1.1
L 5=ESO 28-SC16	0 22 40	−75 04 29	305.42	−41.91	2002 Oct 31	*C*	2400	1.43	1.7
						R	800	1.42	1.5
					2003 Dec 02	*C*	180	1.46	1.3
						R	60	1.47	1.1
L 6=K 4, ESO 28-SC17	0 23 04	−73 40 11	305.67	−43.31	2002 Oct 31	*C*	2400	1.40	1.7
						R	800	1.38	1.5
					2003 Dec 02	*C*	180	1.42	1.3
						R	60	1.43	1.1
L 7=K 5, ESO 28-SC18	0 24 43	−73 45 18	305.49	−43.24	2002 Oct 31	*C*	2400	1.44	1.9
						R	800	1.50	1.6
					2003 Dec 02	*C*	180	1.44	1.3
						R	60	1.45	1.3
L 19=SMC OGLE 3	0 37 42	−73 54 30	304.24	−43.19	2002 Oct 29	*C*	2400	1.46	1.9
						R	800	1.42	1.6
					2002 Oct 30	*C*	240	1.41	1.6
						R	80	1.41	1.2
L 27=K 21, SMC OGLE 12	0 41 24	−72 53 27	303.96	−44.22	2002 Oct 30	*C*	2400	1.36	1.3
						R	800	1.37	1.6
BS 121=SMC OGLE 237	1 04 22	−72 50 52	301.60	−44.25	2002 Oct 30	*C*	2400	1.40	1.8
						R	800	1.44	1.5
HW 47	1 04 04	−74 37 09	301.80	−42.48	2002 Oct 29	*C*	2400	1.41	1.9
						R	800	1.39	1.6
HW 84	1 41 28	−71 09 58	297.22	−45.40	2002 Oct 30	*C*	2400	1.43	1.5
						R	800	1.46	1.7
HW 86	1 42 22	−74 10 24	298.26	−42.49	2002 Oct 31	*C*	2400	1.53	1.9
						R	800	1.50	1.4

Note: [a]cluster identifications are from Kron (1956; K), Lindsay (1958; L), Hodge Wright (1974; HW), Lauberts (1982; ESO), Bica Schmitt (1995; BS) and Pietrzyński et al. (1998; SMC OGLE).

Table 2. Typical photometric errors for a single observation.

ΔT_1 (mag)	$\sigma(T_1)$ (mag)	$\sigma(C-T_1)$ (mag)
13–14	0.005	0.004
14–15	0.005	0.005
15–16	0.010	0.007
16–17	0.010	0.007
17–18	0.012	0.012
18–19	0.026	0.025
19–20	0.045	0.045
20–21	0.080	0.085
21–22	0.160	0.160

Table 3. CCD CT_1 data of stars in the field of L 4. This is a sample of the full table that is available online at http://www.blackwellpublishing.com/products/journals/suppmat/MNR/MNR8694/MNR8694sm.htm

Star	x (pixel)	y (pixel)	T_1 (mag)	$\sigma(T_1)$ (mag)	$C-T_1$ (mag)	$\sigma(C-T_1)$ (mag)	n
...	...	...	...	...	...	...	...
1700	261.580	528.601	18.292	0.003	1.746	0.047	2
1701	1245.357	528.931	19.777	0.005	−0.117	0.035	2
1702	1360.529	530.122	17.864	0.005	1.572	0.002	2
1703	−85.016	530.164	21.974	0.226	−0.201	0.234	1
1704	1821.462	530.196	18.870	0.016	2.114	0.035	1
...	...	...	...	...	...	...	...
...	...	...	...	...	...	...	...
...	...	...	...	...	...	...	...

Notes. (x, y) coordinates correspond to the reference system of Fig. 1. Magnitude and colour errors are the standard deviation of the mean, or else the observed photometric errors for stars with one measurement.

relatively rapid ($\tau \lesssim 3$ Gyr) initial abundance increase followed by a more modest rise starting at ∼10 Gyr and continuing until the present day. As exhibited by their data, with the exception of Lindsay 113 and NGC 339 for which the authors claim anomalously low abundances, the AMR is quite consistent with the predictions of the simple closed box model of chemical evolution.

Other models have been put forward for the chemical evolution of the SMC, paying special attention to the distinct Fe/O and Fe/α ratios, which are generally found to be higher than in Galactic stars with the same metallicity ([Fe/H]). Gilmore & Wise (1991) pointed out that one way to get this effect is to assume distinct star formation bursts, with Type Ia supernovae contributing extra iron during quiescent intervals, and an overall slower star formation rate than that characteristic of the Galaxy. An alternative way to explain low metallicities is to assume outflow, which can be either homogeneous or selective, the latter being associated

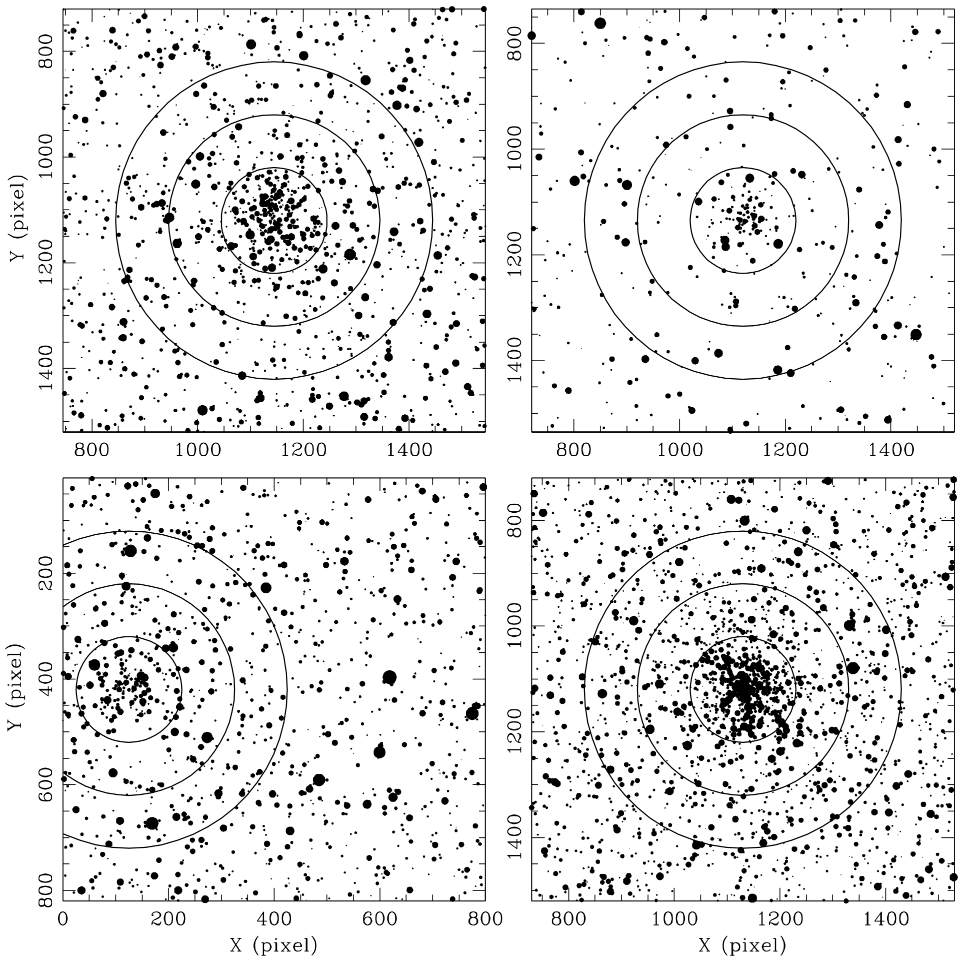

Figure 1. Schematic finding charts for the Small Magellanic Cloud (SMC) cluster fields. (a) L 4 (upper left), L 5 (upper right), L 6 (bottom left) and L 7 (bottom right). (b) L 19 (upper left), L 27 (upper right), BS 121 (bottom left) and HW 47 (bottom right). (c) HW 84 (upper left) and HW 86 (upper right). Three concentric rings are generally shown, corresponding to the circular extractions explained in the text. North is up and east is to the left. The size of the plotting symbol is proportional to the T_1 brightness of the star.

with starbursts and leading to enhancement of the Fe/O ratio (e.g. Marconi, Matteucci & Tosi 1994). With this background, Pagel & Tautvaišienė (1998) included inflow and non-selective galactic winds in their models, and considered both smooth and bursting star formation rates, the latter giving a better fit to the SMC AMR. They also predicted essentially solar abundance ratios for primary elements that appear to fit most of the data within their substantial scatter.

Recently, Bekki et al. (2004) presented results of gas dynamical N-body simulations of the interaction between both Magellanic Clouds, paying special attention to the effect of tidal forces. They found that the very first close encounter between both Magellanic Clouds occurred approximately 4 Gyr ago and was the beginning of a period of strong tidal interaction that likely induced dramatic gas cloud collisions, leading to a strong enhancement of the formation of star clusters sustained until the present. They suggest that this could explain the mysterious Large Magellanic Cloud (LMC) cluster age gap (e.g. Da Costa 1991; Geisler et al. 1997), where only a single cluster is found between ∼12 and 3 Gyr of age. Finally, they argued that the differences between the LMC and SMC cluster AMRs arise from the different birthplaces and masses of the clouds, the SMC being less massive and born nearer to the Galaxy, and consequently more susceptible to Galactic tidal effects, thus allowing possibly more continuous cluster formation and avoiding an SMC cluster age gap.

As can be seen, a variety of models have been developed with different levels of complexity, but the observational data used to constrain their different hypotheses and predictions have been practically the same handful of clusters as those listed by Piatti et al. (2001). There has been a dearth of recent colour–magnitude diagram (CMD) studies of SMC clusters. Therefore, the aim of this paper is to enlarge the sample of well-studied star clusters in the SMC by obtaining CMDs down to below the main-sequence turnoff (MSTO) and thus derive their ages and metallicities. In particular, we will build on our previous work on SMC clusters (Piatti et al. 2001), using the same techniques and allowing us to increase our homogenous data base. We present new Washington C, T_1 photometric observations of 10 unstudied star clusters (Lindsay 4, 5, 6, 7, 19, 27, BS 121, HW 47, 84, and 86) that provide further constraints on the chemical evolution of the SMC. When combined with our previous studies and information from the literature, these new data document the existence of a bursting cluster formation episode that peaked 2–3 Gyr ago. In Section 2, we describe the observations and the guidelines for the data reductions. The analysis of the

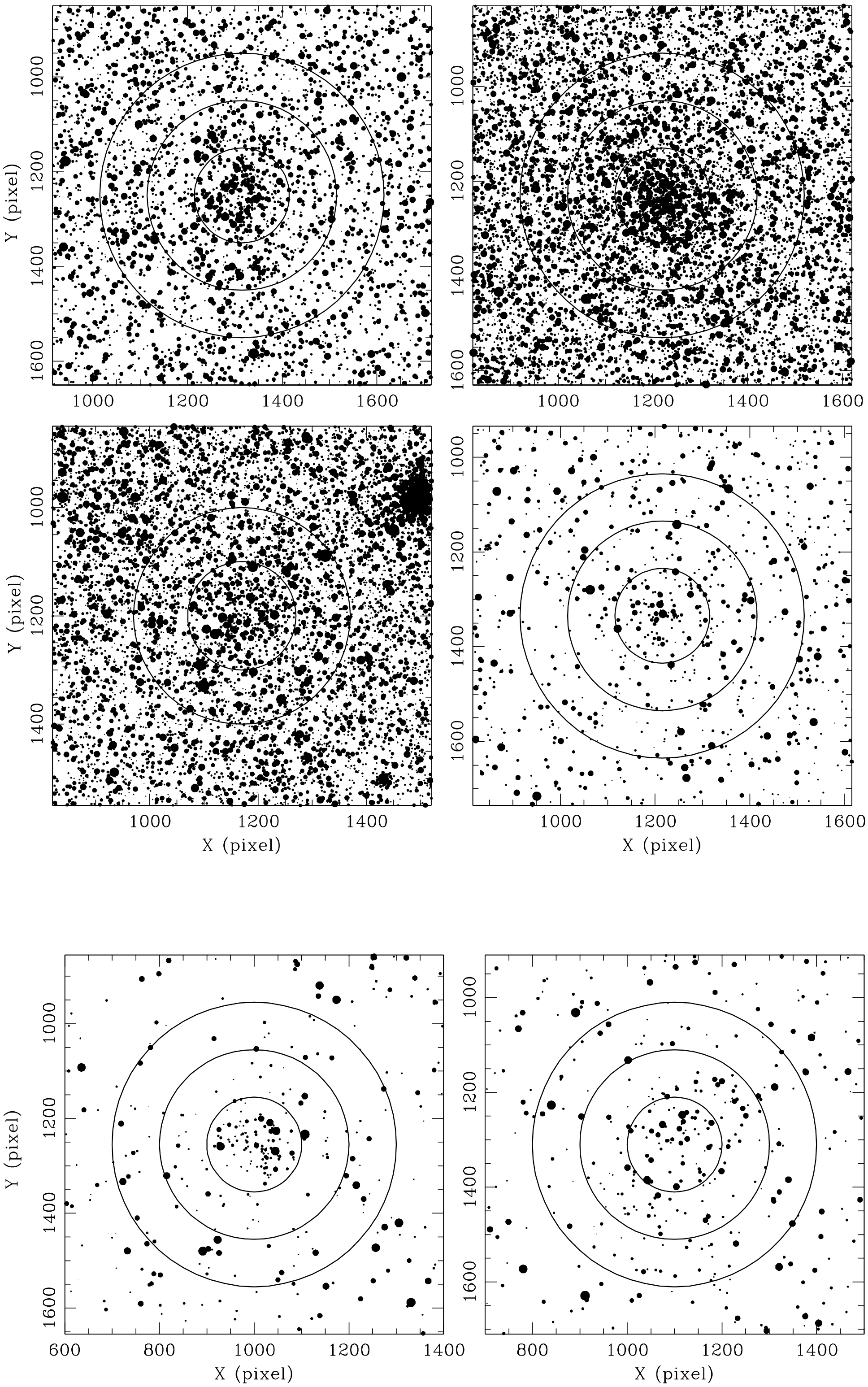

Figure 1 – *continued*

photometric data and the derivation of the cluster fundamental parameters are presented in Section 3, while in Section 4 we discuss the AMR of the SMC in the light of the available observations and chemical evolution models. Finally, we summarize the main conclusions of the paper in Section 5.

2 OBSERVATIONS AND REDUCTIONS

We selected 10 SMC clusters that either had no previous CMDs available, or whose CMD did not reach the MSTO and therefore had little or no information regarding age or metallicity. The observed

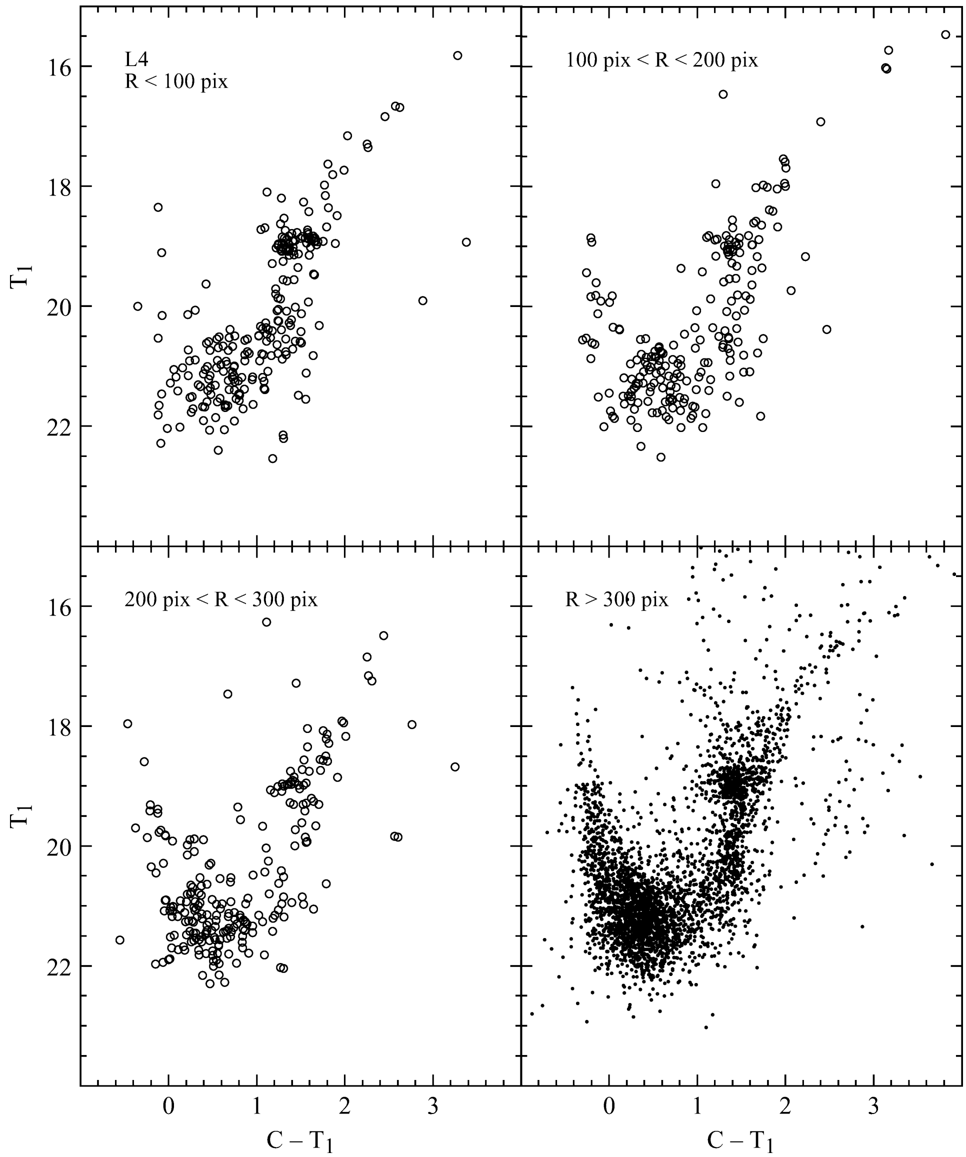

Figure 2. Washington T_1 versus $C - T_1$ colour–magnitude diagrams (CMDs) for all the measured stars in the cluster fields: (a) L 4 ,(b) L 5, (c) L 6, (d) L 7, (e) L 19, (f) L 27, (g) BS 121, (h) HW 47, (i) HW 84 and (j) HW 86. Extraction radii in pixels are given in each panel.

clusters are given in Table 1, which lists their various designations, equatorial and Galactic coordinates, and details of the observations. The only clusters previously observed in any detail are L 19 and 27, for whom Pietrzyński et al. (1998) derive a lower limit of a Gyr for their ages from the Optical Gravitational Lensing Experiment (OGLE) data base.

The 10 SMC cluster fields were observed during four nights with the Cerro Tololo Inter-American Observatory (CTIO) 0.9-m telescope in 2002 October and 2003 December with the Tektronix 2K #3 CCD, using quad-amp readout. The scale on the chip is 0.4 arcsec pixel^{-1} yielding an area covered by a frame of 13.5 × 13.5 arcsec. The integrated IRAF[1]-Arcon 3.3 interface for direct imaging was employed as the data acquisition system. A mean gain of 3 e$^-$/ADU and a mean readout noise of 4.9 e$^-$ resulted for the chosen settings.

[1] IRAF is distributed by the National Optical Astronomy Observatories, which is operated by the Association of Universities for Research in Astronomy, Inc., under contract with the National Science Foundation.

We obtained data with the Washington (Canterna 1976) C and Kron–Cousins R filters. The latter has been shown to be an efficient substitute for the standard Washington T_1 filter (Geisler 1996). Single exposures of 40 min in C and 800 s in R_{KC} were taken for each field. Additional short calibration exposures were taken on photometric nights for the clusters originally observed during non-photometric conditions. Their airmasses were always $\lesssim$1.5 and the seeing was typically ∼1.5 arcsec. The observations were supplemented with nightly exposures of bias, dome- and (when appropriate) twilight sky-flats to calibrate the CCD instrumental signature.

Two of the nights (2002 October 30 and 2003 December 2) were photometric. On each photometric night, a large number (typically 20) of standard stars from the list of Geisler (1996) were also observed. Care was taken to cover a wide colour and airmass range for these standards in order to calibrate the program stars observed on these nights properly.

The data were processed at the Physics Department of the University of Concepción (Chile) and at the Institute for Astronomy and

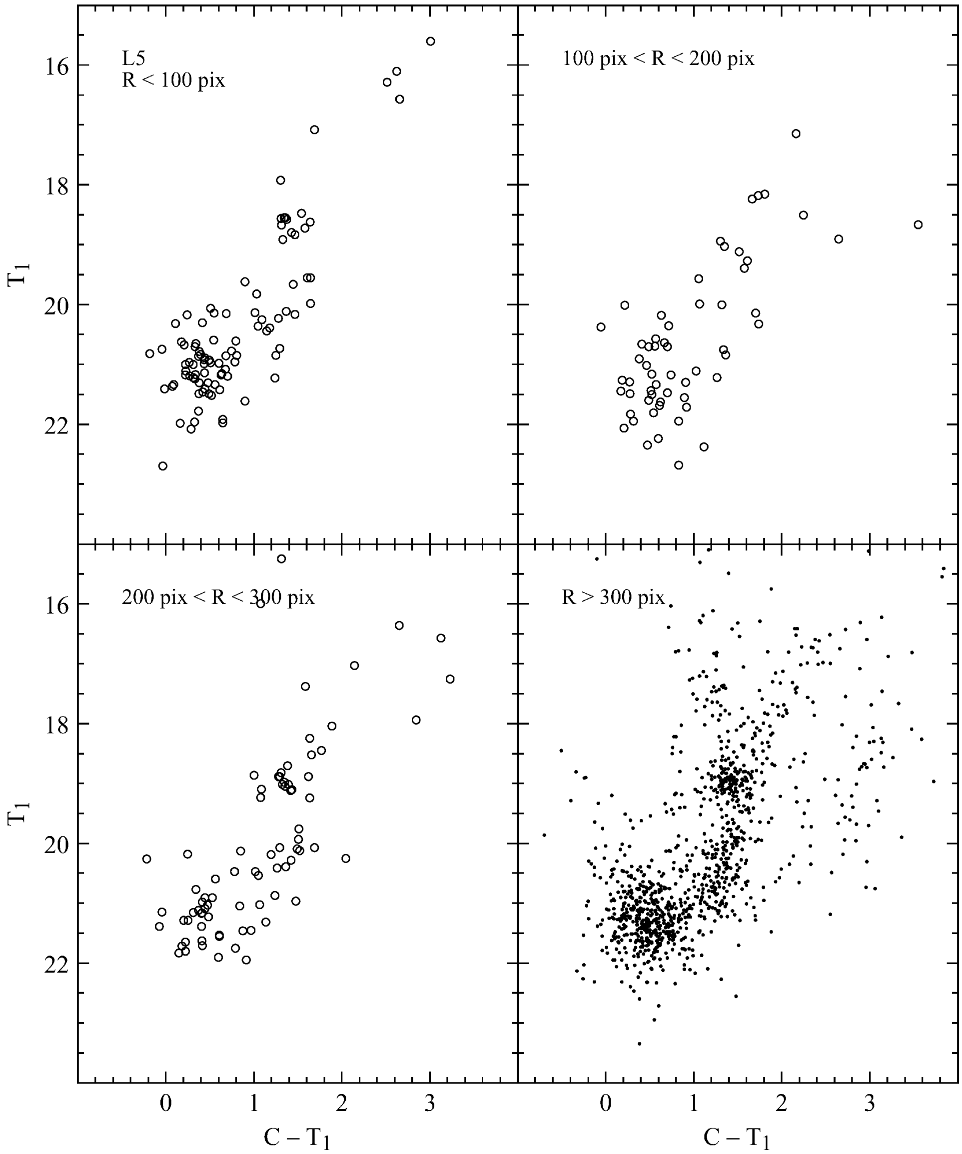

Figure 2 – *continued*

Space Physics (Argentina) using the QUADPROC package in IRAF. After applying the overscan-bias subtraction for the four amplifiers independently, we carried out flat-field corrections using a combined sky-flat frame, which was previously checked for a non-uniform illumination pattern with the averaged dome-flat frame. Then, we performed aperture photometry for the standard stars observed on 2002 October 30 (18 stars) and on 2003 December 2 (23 stars) using the APPHOT task within IRAF. The relationships between instrumental and standard magnitudes were obtained by fitting the equations

$$c = a_1 + T_1 + (C - T_1) + a_2 X_C + a_3 (C - T_1), \quad (1)$$

$$r = b_1 + T_1 + b_2 X_R + b_3 (C - T_1), \quad (2)$$

where a_i and b_i (i = 1, 2 and 3) are the coefficients derived through the FITPARAM routine in IRAF and X represents the effective airmass. Capital and lower-case letters represent standard and instrumental magnitudes, respectively. We first solved for all three transformation coefficients simultaneously (using the PHOTCAL package in IRAF) for the nights of 2002 October 30 and 2003 December 2 and found mean colour terms of -0.110 ± 0.013 in c and $-0.0.24 \pm 0.005$ in r for both nights. Averaged values were 3.261 ± 0.031 and 2.948 ± 0.024 for the c and r zero points, while typical airmass coefficients resulted in 0.41 and 0.16 for c and r, respectively. The nightly rms errors from the transformation to the standard system were 0.017 and 0.013 mag for c and r, respectively, indicating these 2 nights were of excellent photometric quality.

Point spread function (PSF) photometry was performed for all the cluster fields using the stand-alone version of the DAOPHOT II package (Stetson 1994). We refer the reader to the work of Piatti et al. (1999) for a more detailed description about how we obtained the final cluster instrumental photometry. The standard magnitudes and colours for all the measured stars of the clusters observed on 2002 October 30 and 2003 December 2 were computed by inverting equations (1) and (2). For the remaining cluster observations, obtained on the non-photometric nights of 2002 October 29 and 31, we transformed their instrumental magnitudes and colours to the standard ones obtained from the short calibration observations taken on the photometric nights. This allowed us not only to

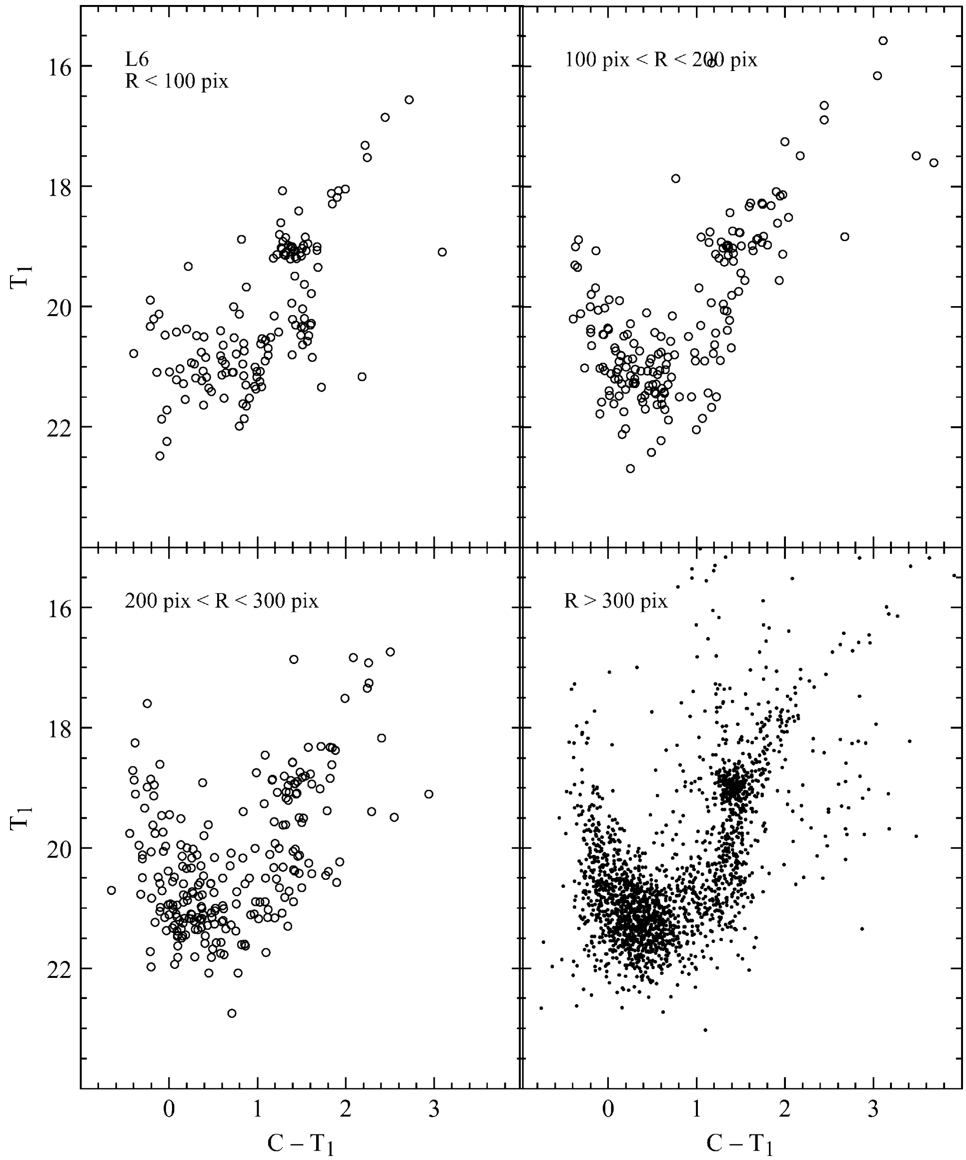

Figure 2 – *continued*

average magnitudes and colours for many stars observed twice but also to include in the master tables all the stars observed once. In the cases of HW 47 and 86, we transformed the instrumental magnitudes and colours to standard values through the relations that arise for L 19 between the nights of 2002 October 29 and 30, and for L 7 between the nights of 2002 October 29 and 2003 December 2, respectively. These relations resulted within the errors to be the same as those derived for L 4, 5 and 6 between the nights of 2002 October 31 and 2003 December 2, and for L 34 and H86-70 (young SMC clusters) between 2002 October 29 and 30. Table 2 gives typical photometric (internal DAOPHOT) errors for selected magnitudes. We generated a master table per cluster containing a running number, the *x* and *y* coordinates, the T_1 magnitudes and $C - T_1$ colours, the observational errors $\sigma(T_1)$ and $\sigma(C - T_1)$ and the number of observations. These tables were built by combining all the independent measurements using the stand-alone DAOMATCH and DAOMASTER programmes kindly provided by Peter B. Stetson. Tables 3 to 12 give this information. Only a portion of Table 3 is shown here, for guidance regarding its form and content; the whole content of Table 3 is available in the on-line version of the journal on Synergy (as are Tables 4-12), at http://www.blackwellpublishing.com/products/journals/suppmat/MNR/MNR8694/MNR8694sm.htm. These values are only representative and vary with cluster and field crowding, seeing, etc.

Fig. 1 shows the schematic finding charts built using all the measured stars in each cluster. The size of the plotting symbol is proportional to the T_1 brightness of the star.

3 ANALYSIS OF THE COLOUR–MAGNITUDE DIAGRAMS

Fig. 2 shows radial CMDs in the region of each program cluster. A radial bin size of 100 pixel has been applied. Four bins are shown: an inner bin (<100 pixel), two intermediate bins (100–200 and 200–300 pixel) and an outer bin (>300 pixel). In each case, the inner diagram clearly shows the features of the CMD of the cluster. In particular, each cluster exhibits a red giant branch (RGB), core

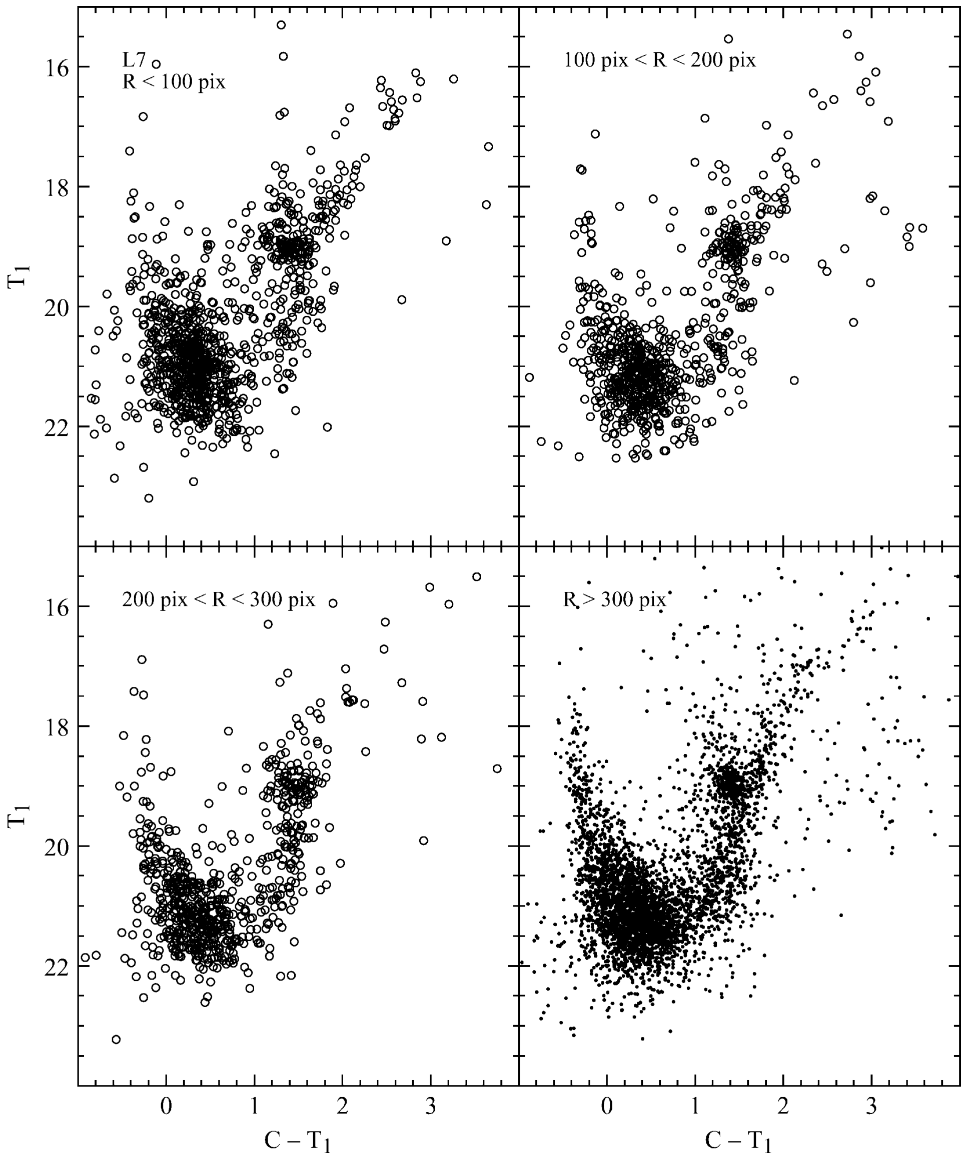

Figure 2 – *continued*

helium burning red clump (RC) stars, a subgiant branch (SGB) and a distinct increase in the numbers of stars in the MSTO region and fainter. The MSTOs generally lie some 0.5–1.25 mag above the limit of our photometry, allowing us to derive reasonable MSTO ages. The one exception to this is L 6, which does not show a well-defined MSTO. In addition, the RGBs of L 5, HW 47, 84 and 86 are sparsely populated. Most cluster CMDs also show some bright main sequence (MS) stars above the apparent turn-off (TO), which are almost certainly young SMC field stars superimposed on the cluster, as evidenced by the field CMDs (outermost region).

We are primarily interested in determining the age and metal abundance of each cluster in our sample. In order to maintain consistency, we have utilized the same techniques to measure these quantities as in our previous paper on SMC clusters (Piatti et al. 2001). First, we adopt a distance modulus of $(m - M)_V = 19.0$ (Cioni et al. 2000) along with the following equations: $E(C - T_1) = 1.97E(B - V)$ and $M_{T_1} = T_1 + 0.58E(B - V) - (m - M)_V$; from Geisler & Sarajedini (1999). The reddening values are taken both from the Burstein & Heiles (1982, hereafter BH) and Schlegel, Finkbeiner & Davis (1998, SFD) extinction maps. In general, reddening estimates differ in 0.01–0.02 mag, except for L 5, HW 47 and 86 whose differences are between 0.06 and 0.10 mag; the BH values being higher. We adopted the smaller values.

The ages are calculated by determining the difference in T_1 magnitude between the RC and the MSTO displayed in Fig. 2 and using equation (4) of Geisler et al. (1997) to compute the age. Note that this age measurement technique does not require absolute photometry. The metallicities have been estimated by comparing the cluster RGBs with the standard fiducial globular cluster RGBs from Geisler & Sarajedini (1999). This derived metallicity is then corrected for age effects via the prescription given in Geisler et al. (2003). We note that ages and metallicities determined in this way have been found to be in good agreement with those derived from comparison to appropriate theoretical isochrones (e.g. Geisler et al. 2003; Piatti et al. 2003a,b).

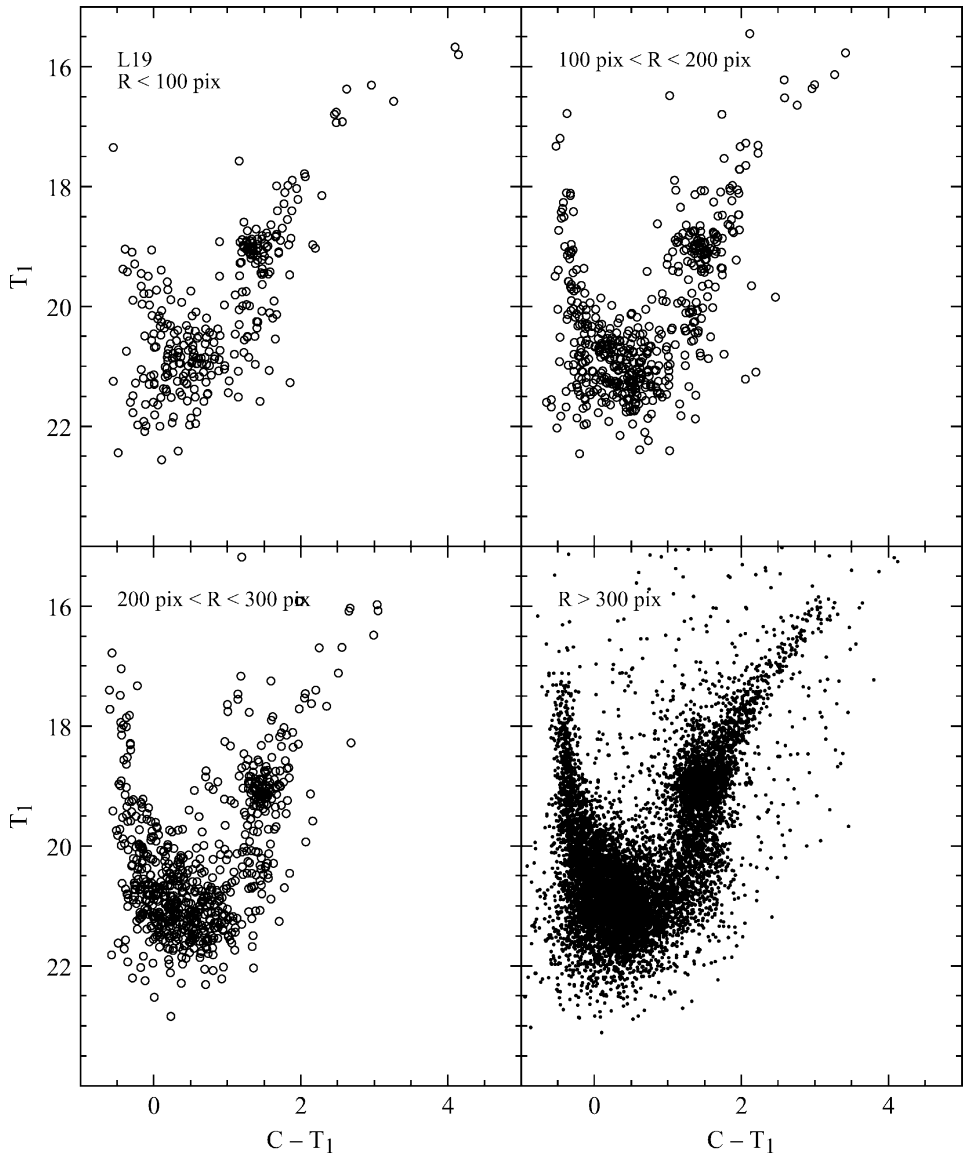

Figure 2 – *continued*

In general, we used each of the two innermost CMDs to derive both ages and metallicities. The innermost bin is less contaminated by the surrounding field but also more crowded and with larger errors, while the second bin is generally still dominated by cluster stars. The mean δT_1 values and their errors were estimated from the average of independent measurements by two authors. The maximum difference in δT_1 was only 0.3 mag and the mean difference was 0.12 ± 0.12 mag.

The cluster and field RCs have an average magnitude of $T_{1_{\rm clump}} \approx 19.0 \pm 0.1$mag, as expected for objects at the distance of the SMC (see Piatti et al. 2001), with two exceptions: both the cluster and field CMDs of HW 84 and 86 have RCs that appear to be brighter, by ~0.3–0.5 mag. Although these are the sparest CMDs and most difficult to derive accurate RC mag values for, these values are clearly brighter than for the other objects. These are the two easternmost regions of the SMC in our sample, some 3° east of the optical centre. We note that L 113 is some 0.3° further east (and ~0.5° north from HW 86) and is a SMC cluster. Crowl et al. (2001) noted that the statistically significant range of distances among the populous clusters indicates that the SMC does indeed exhibit a substantial extent in the line-of-sight (LOS) direction. They have obtained a $\pm$ 1σ depth between ~6 and ~12 kpc, which is consistent with the values quoted by Gardiner & Hawkins (1991), which lie anywhere between 4 and 16 kpc, depending on which portion of the SMC one is observing. HW 84 and 86 are between ~4 and ~7 kpc, just within the SMC cluster LOS depth range.

Table 13 gives our derived reddening, age and metallicity information for the clusters. We find that all clusters are of intermediate age, lying between ~1.5–4 Gyr. The errors in the metallicities and ages have also been estimated. The latter includes the combined photometric error of stars at the RC and the MSTO converted to an age error using equation (4) of Geisler et al. (1997). We estimate the errors in the ages to be of the order of 0.2 Gyr for the younger clusters and up to 0.9 Gyr for the older clusters (given the non-linearity of the δT_1–age relation), with a typical error of 0.5 Gyr. The metallicity errors were estimated taking into account both the

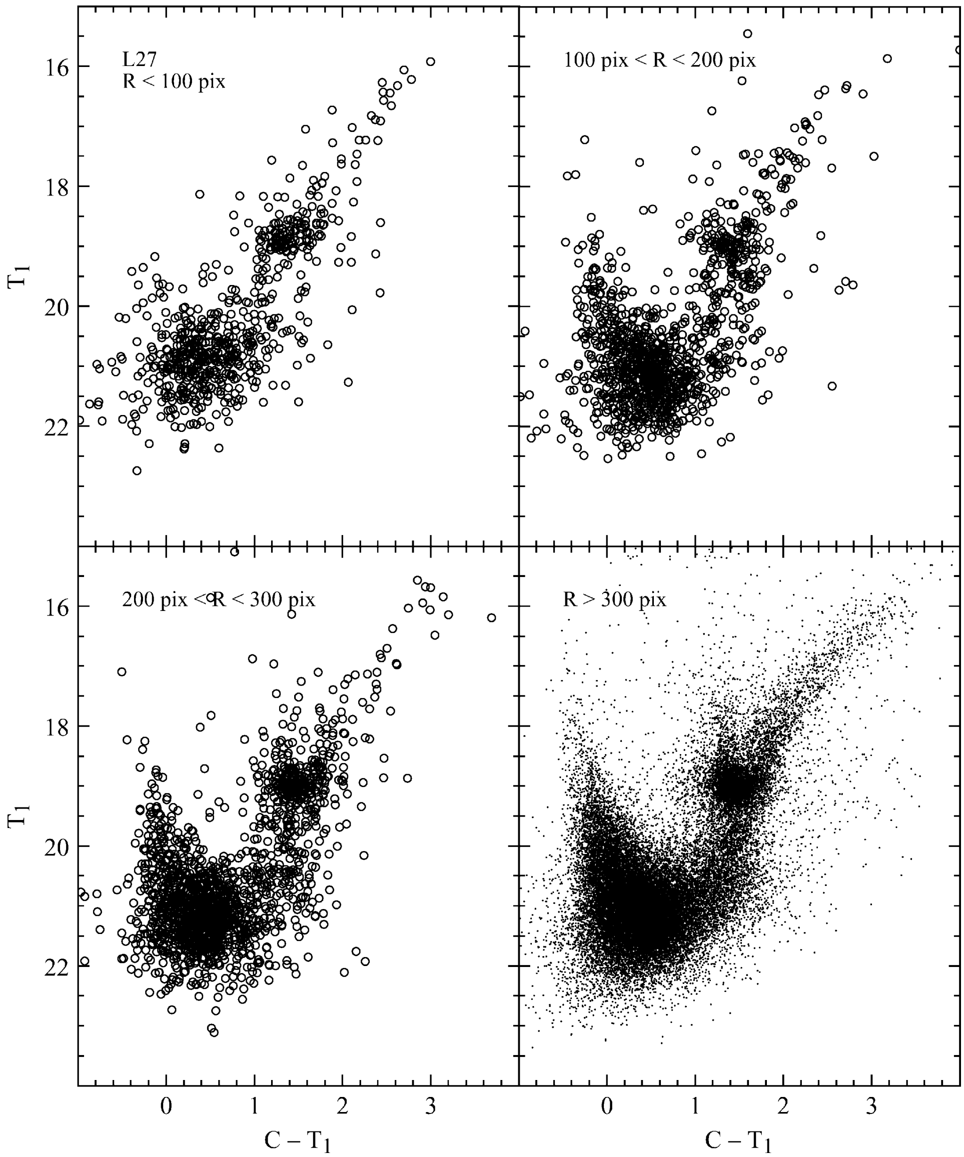

Figure 2 – *continued*

dispersion of the RGB stars and the separation between the defined isoabundance lines in the M_{T_1} versus $(C - T_1)_o$ plane; adopting larger errors for clusters with few stars. We note that an increase of the assumed reddening by $E(B - V) = 0.03$ decreases the derived metallicity by 0.12 dex (Bica et al. 1998).

4 DISCUSSION

Fig. 3 shows the distribution of the 10 studied clusters with relation to the SMC bar and the optical centre, represented by a straight line and a cross, respectively. We assume for the position (J2000) of the optical centre: RA $00^h52^m45^s$, Dec. $-72°49'43''$ (Crowl et al. 2001). In addition, with the aim of performing a more complete analysis of the age and metallicity of the clusters and the chemical evolution of the SMC, we added to our sample the 16 clusters compiled by Piatti et al. (2002), which have ages and metallicities put on to a similar scale as those obtained in the present study. As far as we are aware, the full sample of 26 clusters is the largest sample of SMC clusters with ages and metallicities placed on homogeneous scales. In particular, we have nearly tripled the number of well-studied clusters with ages between ~1 and ~5 Gyr. The clusters in the new sample are mainly located in the southern half of the SMC, with a mean total number of clusters per quadrant of 6 ± 1 objects (the common apex of the four quadrants is at the selected optical centre).

The distributions of cluster ages and metallicities along the right ascension and declination axes are depicted in Fig. 4. The upper left panel shows that the 10 clusters in the present study were born within a relatively small age range of ~2.5 Gyr, which represents ~20 per cent of the lifetime of the SMC. They also appear mostly spread across the whole extension (right ascension coordinate) of the SMC cluster system. On the other hand, the upper right panel shows them located mostly south of the SMC optical centre. Including the additional clusters (open triangles), it seems that there is no evidence for any kind of age structure across the SMC field, because one finds younger and older clusters at any position. Note that we are excluding the SMC bar, where clusters younger than 1 Gyr are found abundantly (see, e.g. Rafelski & Zaritsky 2005). We do confirm the same tendency hinted at in Crowl et al. (2001) for clusters to

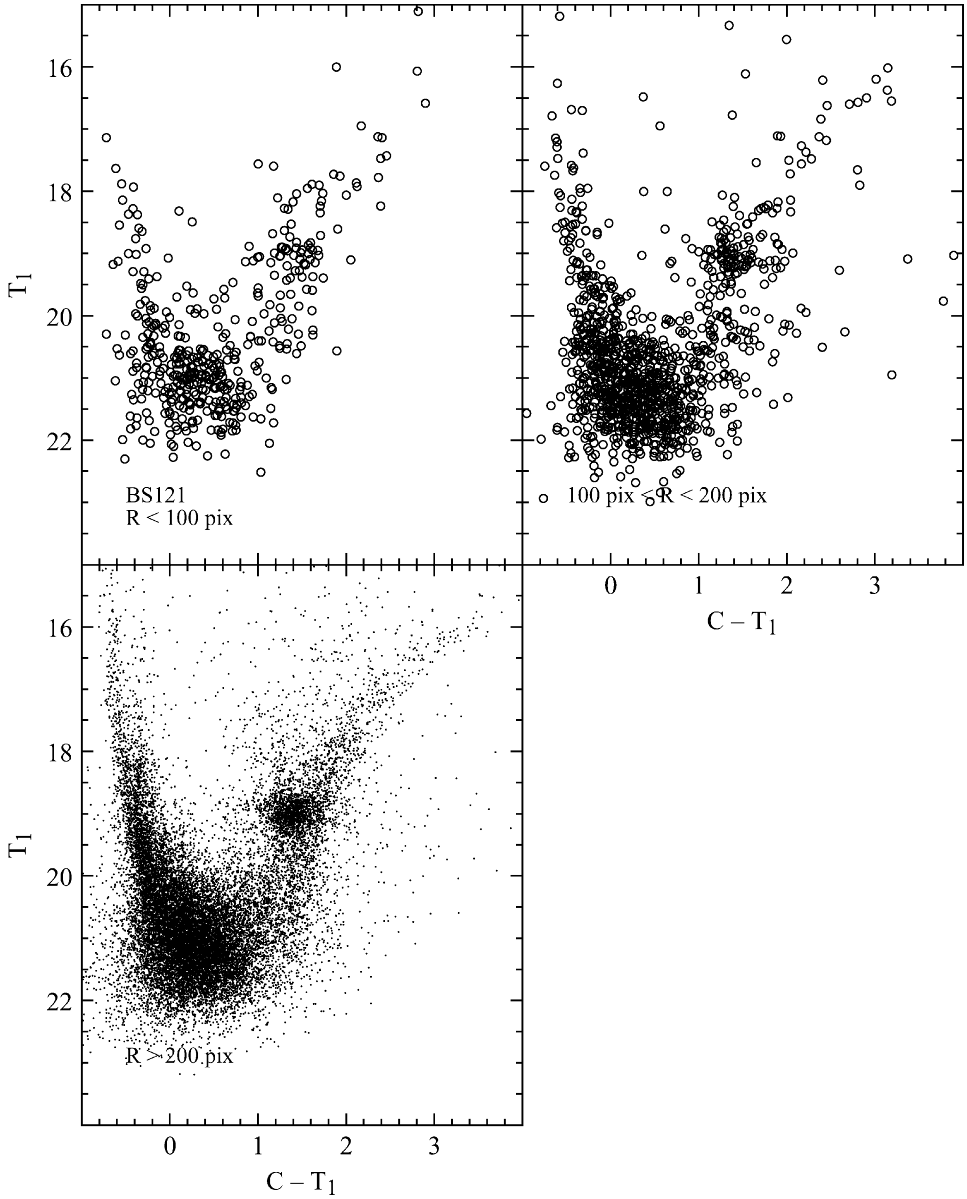

Figure 2 – *continued*

be slightly younger in the eastern half, but this result is still very preliminary. The lower left and right panels reveal that the 10 studied clusters have metal abundances from values as metal poor as −1.3 dex up to ones as metal rich as −0.6 dex. This metallicity range also overlaps that of the additional 16 clusters (open triangles). One finds metal-poor and metal-rich objects at virtually any location in the observed (projected) volume of the SMC star clusters. We do not see any indication of the Crowl et al. (2001) suggestion for metallicities to be higher in the east. From a chemical evolution point of view, these results lead us to conclude that the SMC has remained largely inhomogeneous (with gas that is not well mixed) from its birth until approximately 1 Gyr ago. In particular, from one side to the other of the galaxy, it is possible to find clusters born 2–3 Gyr ago with similar metallicities. Curiously, this happens for the whole range of metal abundances.

We computed the angular separations of the clusters with respect to the SMC optical centre (last column of Table 13) and constructed Fig. 5, which shows at the top the radial distribution of cluster ages and metallicities. There is apparently little correlation between cluster age and radial position in the SMC. With the exception of the oldest cluster, NGC 121, at a distance of $\sim 2\overset{\circ}{.}5$ from the optical centre of the SMC, all radial locations between $\sim 0\overset{\circ}{.}8$ and $\sim 4^\circ$ harbour clusters covering the intermediate-age range of ∼1 to ∼9 Gyr.

Keeping in mind that our cluster sample suffers from substantial incompleteness, particularly for clusters younger than 1 Gyr, the lower left panel of Fig. 5 suggests that the SMC clusters exhibit a bursting formation history with one episode occurring ∼2.5 Gyr ago and another possibly occurring ∼6.5 Gyr ago. This is consistent with the work of Rich et al. (2000) who studied a relatively small sample of seven SMC clusters and found that they congregated in two age bins: one at 2 ± 0.5 Gyr and another at 8 ± 2 Gyr. These results are supported by the work of Bekki et al. (2004), who showed that both Magellanic Clouds have suffered mutual tidal interactions. From gas dynamical *N*-body simulations of the evolution of the LMC and

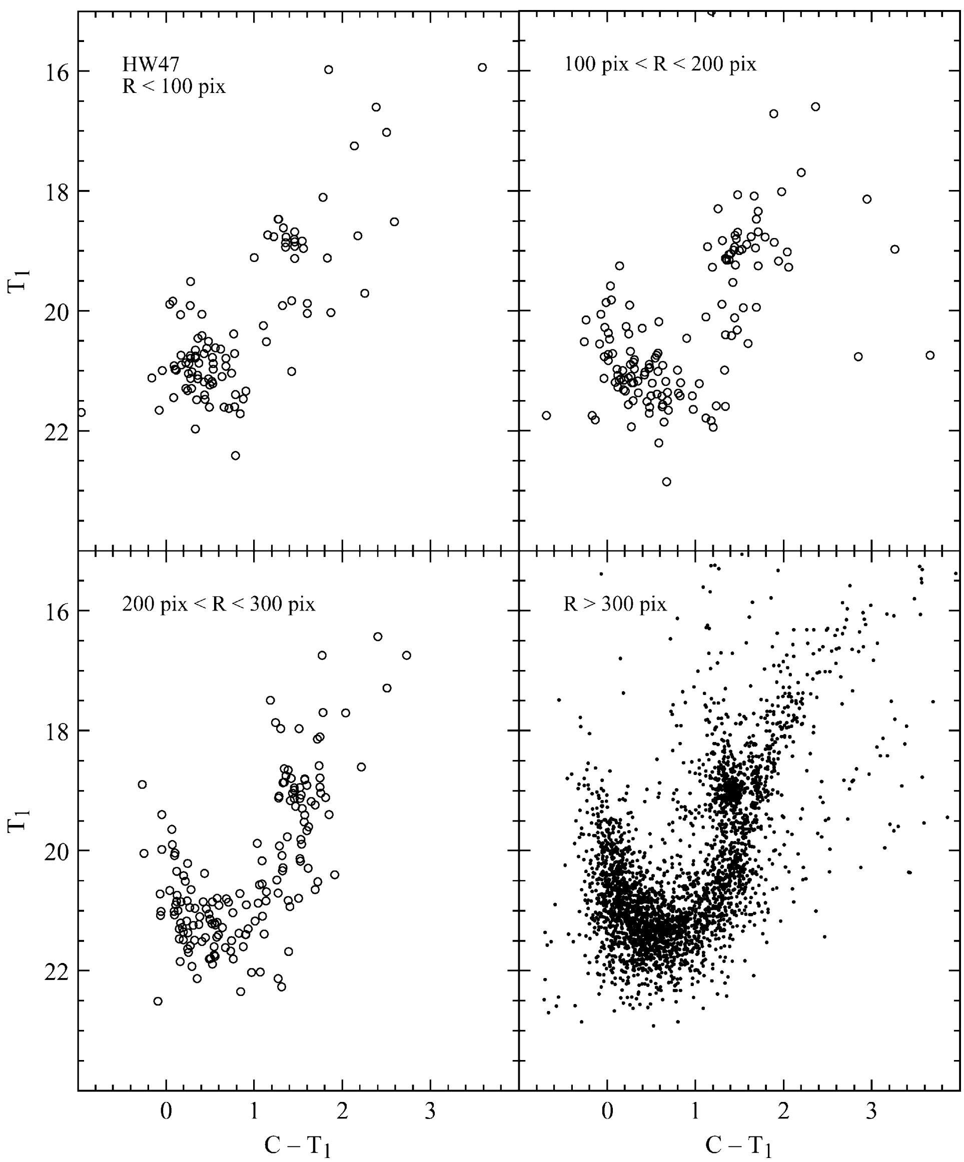

Figure 2 – *continued*

SMC in the context of their Galactic orbits and mutual interactions, they found that the first very close encounter between the clouds occurred ∼3.6 Gyr ago, with a separation of only approximately 10 kpc, much smaller than their previous typical separation. This first close passage initiated a period of strong tidal interaction, which is still occurring and that most likely induced dramatic gas cloud collisions. Such collisions trigger the formation of a large number of star clusters, which has been sustained by strong tidal interactions ever since. For example, a second very close passage occurred approximately 2.8 Gyr ago. Bekki et al. (2004) use this model to account for the LMC cluster age gap (the lack of clusters between 3 and 12 Gyr) and especially to explain the large number of clusters formed starting approximately 3 Gyr ago. They only briefly interpret their model implications for the distribution of SMC cluster ages. They used one of our previous age compilations (Piatti et al. 2002), which did not show any strong age concentrations, and argued that the SMC was most likely born closer to the Galaxy and, being less massive, was much more influenced by Galactic tides, which have generally been sufficient to trigger massive cluster formation throughout the lifetime of the SMC, with no preferred epochs. However, both Piatti et al. (2001) and Rich et al. (2000) suggest several preferred cluster epochs, with Piatti et al. suggesting ∼3 and 6 Gyr. Our new data adds substantially to the total number of cluster ages available and does indeed appear peaky. Note that the large peak at approximately 2.5 Gyr would be in excellent accord with the Bekki et al. (2004) prediction for enhanced cluster formation at this epoch as a result of a very close passage between the two clouds, but now in reference to the enhanced formation of SMC clusters, as well as for their counterparts in the LMC. We believe that this explanation appears to be a very reasonable one and merits further attention. The reason for the older peak remains unexplained. However, note that there was quite a close passage approximately 5.3 Gyr ago that may be related. Clearly, the sample size, age resolution and incompleteness effects, combined with the uncertainties inherit in the orbits and their modelling, makes these only interesting suggestions at the current time.

The metallicity distribution function (MDF) in the lower right panel of Fig. 5 shows that the most frequent cluster metal

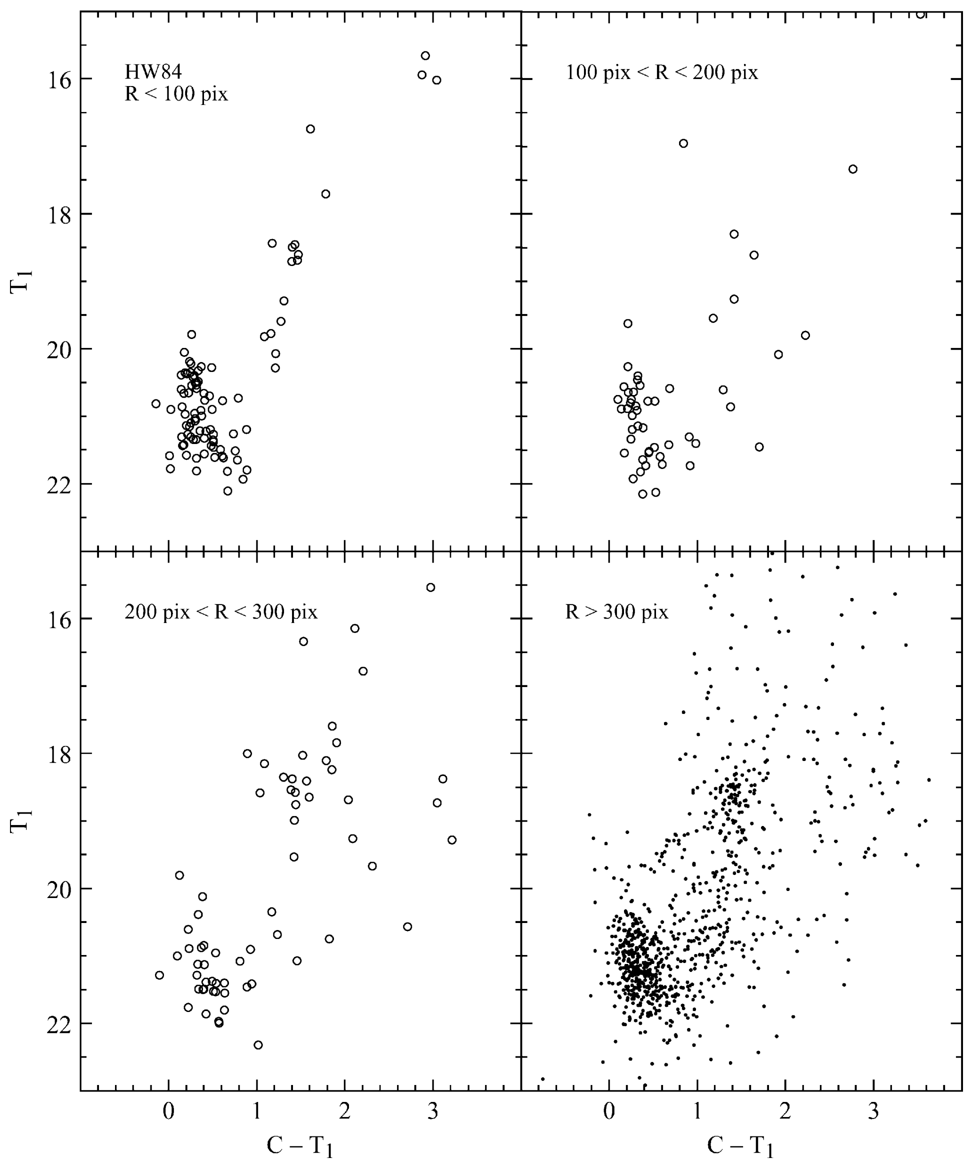

Figure 2 – *continued*

abundance value is -1.25 ± 0.10 dex, but that there also exists a handful of clusters with metallicities around -0.8 dex reminiscent of a bimodal metallicity distribution. We note that the clusters born during the bursting formation event at $\sim$2–3 Gyr ago have a range of metallicities implying that a chemical abundance inhomogeneity was present in the SMC at that time.

Some clues towards a better understanding of the age and metallicity distributions of Fig. 5 (lower panels) can be discerned from the analysis of Fig. 6. There, we show the AMR constructed from the enlarged sample of 26 star clusters. We have also overplotted two star formation models for comparison purposes. The solid line represents the bursting star formation history of Pagel & Tautvaišienė (1998), whereas the dashed line depicts a simple closed system with continuous star formation under the assumption of chemical homogeneity (Da Costa & Hatzidimitriou 1998). The burst is assumed to have occurred at 3 Gyr, in good agreement with our findings above. The appearance of Fig. 6 further supports the bursting star formation model as the most probable paradigm to describe the SMC. Indeed, the incipient evidence of a bursting formation episode in fig. 11 of Piatti et al. (2001) is here confirmed by a more complete cluster sample, especially for clusters with ages of 2–3 Gyr. The range of metallicities of these young-burst clusters could help to theoretically constrain the ability of a bursting episode to chemically enrich the interstellar medium. On the other hand, more cluster observations are needed to find the relation, if any, between the metallicity distribution of the cluster and the bursting formation episodes, because neither of the metallicity peaks in the lower right panel of Fig. 5 ([Fe/H] = -1.25 and -0.8) corresponds to any meaningful bursting feature in Fig. 6.

5 SUMMARY

New Washington photometry was presented for 10 previously unstudied (or poorly studied) star clusters projected on to the SMC body and its outskirts. We derive CMDs to well below the MSTO in all clusters and determine ages by means of the magnitude difference between the red giant clump and the MSTO, and metallicities from the RGB locus. All clusters turned out to be of intermediate

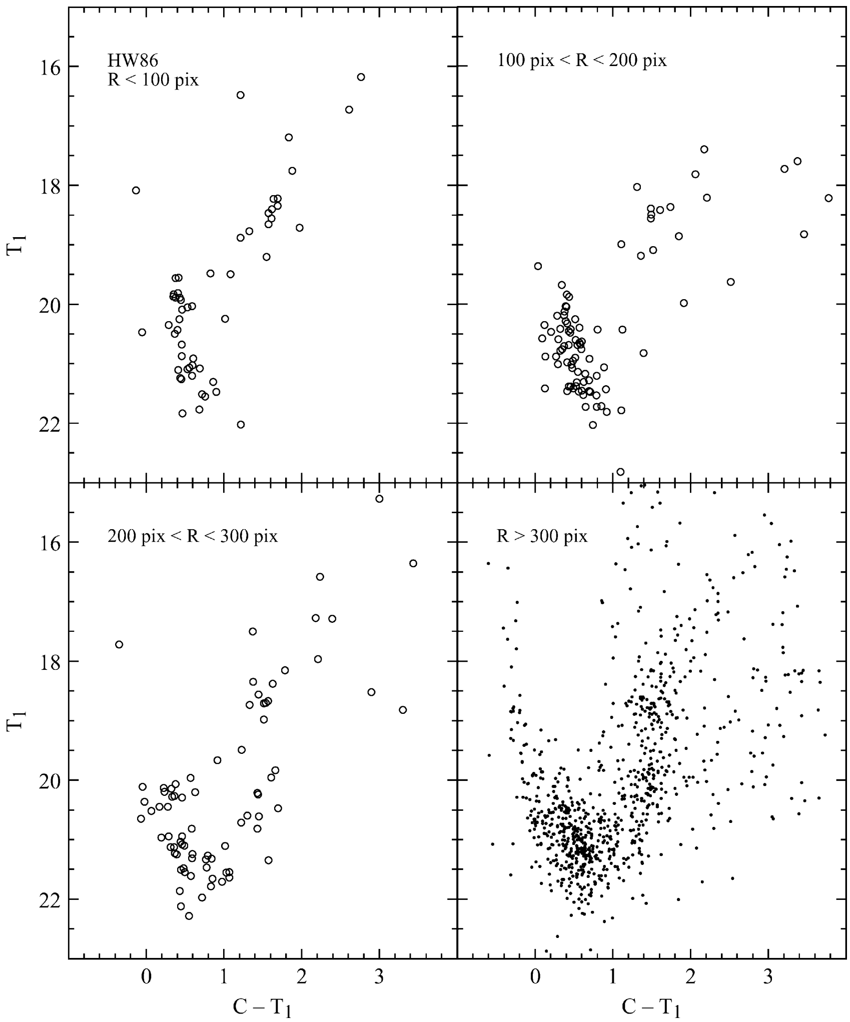

Figure 2 – *continued*

Table 13. Fundamental parameters of SMC clusters.

Name	$E(B-V)$	$\delta(T_1)$ (mag)	Age (Gyr)	$\langle$[Fe/H]$\rangle^a$	R (°)
L 4	0.04	2.1	3.1	-0.9 ± 0.2	2.43
L 5	0.04	2.4	4.1	-1.2 ± 0.2	3.06
L 6	0.03	2.2	3.3	-0.9 ± 0.2	2.30
L 7	0.02	1.7	2.0	-0.6 ± 0.2	2.22
L 19	0.02	1.7	2.1	-0.75 ± 0.2	1.52
L 27	0.11	1.7	2.1	-1.3 ± 0.3	0.84
BS 121	0.14	1.8	2.3	-1.2 ± 0.4	0.86
HW 47	0.05	2.0	2.8	-1.0 ± 0.4	1.96
HW 84	0.03	1.9	2.4	-1.2 ± 0.4	4.11
HW 86	0.04	1.3	1.6	-0.75 ± 0.4	3.76

Note. [a]Metallicities were corrected according to fig. 6 of Geisler et al. (2003). See Section 3 for details.

age, with ages in the range 1.5–4 Gyr and metallicities between $-1.3 <$ [Fe/H] < -0.6. The errors in our ages are themselves age-dependent, ranging from 0.2 Gyr for the youngest clusters to up to 0.9 Gyr for the oldest. For the metallicities, our typical uncertainty is 0.3 dex.

The two easternmost clusters, HW 84 and 86, appear to be closer to us than the bulk of the SMC. This study increases substantially the

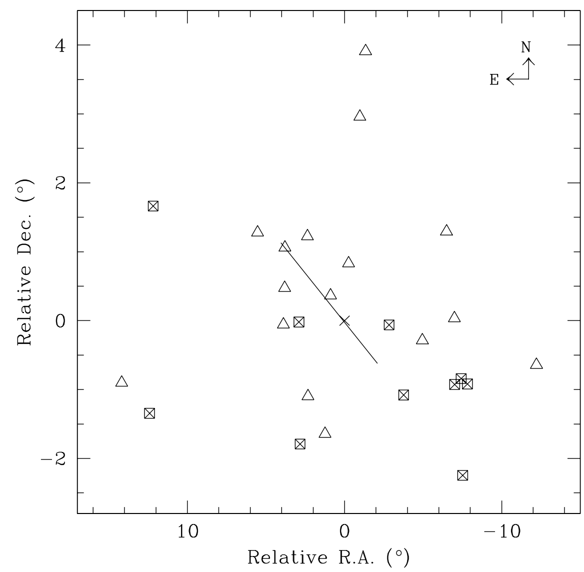

Figure 3. The position of the 10 studied cluster fields (crossed boxes) in relation to the Small Magellanic Cloud (SMC) bar (straight line) and optical centre (cross). Clusters included in Piatti et al. (2002) are also shown as open triangles.

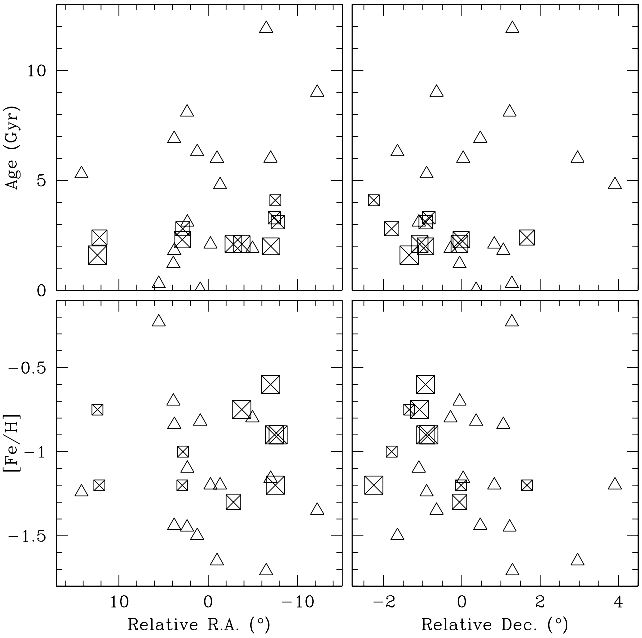

Figure 4. Variation of cluster age (top) and metallicity (bottom) as a function of relative right ascension (left) and declination (right). Symbols are as in Fig. 3. The sizes of the crossed boxes are inversely proportional to the age and metallicity errors.

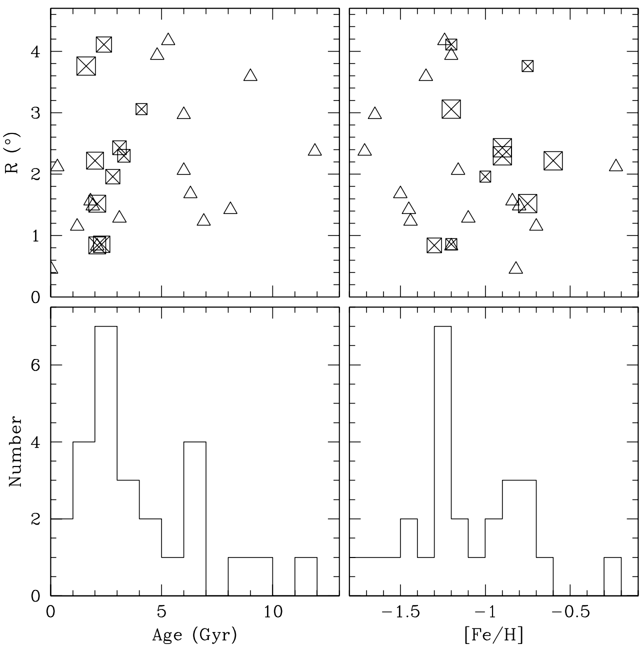

Figure 5. Radial distributions (top) and histograms (bottom) for Small Magellanic Cloud (SMC) cluster ages (left) and metallicities (right). Symbols are as in Fig. 3. The sizes of the crossed boxes are inversely proportional to the age and metallicity errors.

sample of intermediate-age clusters in the SMC with well-derived parameters. We combine our results with those for other clusters in the literature to derive as large and homogeneous a data base as possible (totalling 26 clusters) in order to study global effects. We find evidence for two peaks in the age distribution of SMC clusters,

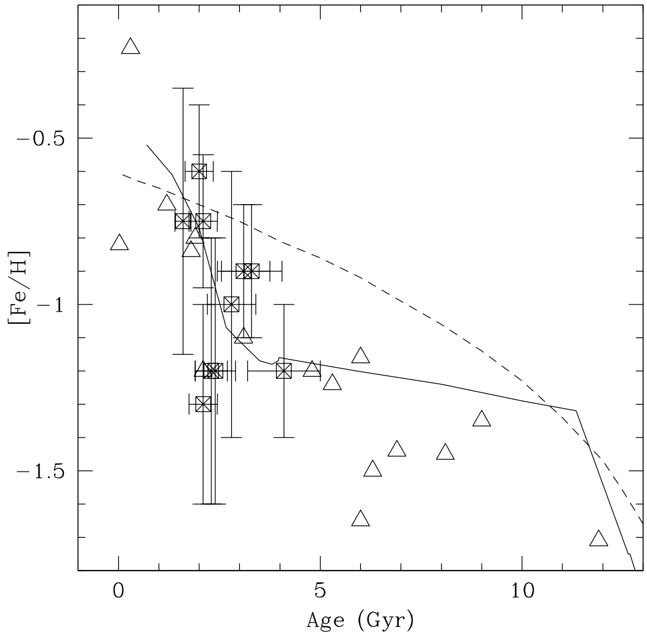

Figure 6. Age–metallicity relationship (AMR) for star clusters in the Small Magellanic Cloud (SMC). Symbols are as in Fig. 3. The data are compared with the closed box continuous star formation model (dashed line) computed by Da Costa & Hatzidimitriou (1998) for an assumed present-day metallicity of −0.6 for the SMC and the bursting model (solid line) of Pagel & Tautvaišienė (1998).

at ∼6.5 and 2.5 Gyr, in good agreement with previous hints involving smaller samples.

A recent theoretical paper by Bekki et al. (2004) studied the dynamics of the LMC/SMC/Galaxy and their interaction via *N*-body simulations. They find evidence that the first very close encounters of the two clouds occurred ∼2.8 and 3.6 Gyr ago and argue that these encounters gave rise to enhanced cluster formation, thus accounting for the famous LMC cluster age gap. Our data suggest that these encounters may also very well have been responsible for a similar epoch of preferred cluster formation in the SMC.

We also find very good agreement between cluster ages and metallicities and the prediction from a bursting model from Pagel and Tautvaišienė with a burst that occurred 3 Gyr ago. These two lines of evidence together favour a bursting cluster formation history as opposed to a continuous one for the SMC.

ACKNOWLEDGMENTS

This work was partially supported by the Argentinian institutions CONICET and Agencia Nacional de Promoción Científica y Tecnológica (ANPCyT). This work is based on observations made at CTIO, which is operated by AURA, Inc., under cooperative agreement with the NSF. We would like to thank the SMARTS consortium for their help and proficiency in obtaining part of these data. We also thank an anonymous referee whose comments helped us to improve the manuscript. DG gratefully acknowledges support from the Chilean Centro de Astrofísica FONDAP No. 15010003.

REFERENCES

Bekki K., Couch W. J., Beasley M. A., Forbes D. A., Chiba M., Da Costa G. S., 2004, ApJ, 610, L93

Bica E., Geisler D., Dottori H., Clariá J. J., Piatti A. E., Santos J. F. C., Jr, 1998, AJ, 116, 723

Burstein D., Heiles C., 1982, AJ, 87, 1165

Bica E., Schmitt H. R., 1995, ApJS, 101, 41

Canterna R., 1976, AJ, 81, 228

Cioni M. R., van der Marel R. P., Loup C., Habing H. J., 2000, A&A, 359, 601

Crowl H. H., Sarajedini A., Piatti A. E., Geisler D., Bica E., Clariá J. J., Santos J. F. C., Jr, 2001, AJ, 122, 220

Da Costa G. S., 1991, in Haynes R., Milne D., eds, Proc. IAU Symp. 148, The Magellanic Clouds. Kluwer, Dordrecht, p. 183

Da Costa G. S., Hatzidimitriou D., 1998, AJ, 115, 1934

Gardiner L. T., Hawkins M. R. S., 1991, MNRAS, 251, 174

Geisler D., 1996, AJ, 111, 480

Geisler D., Sarajedini A., 1999, AJ, 117, 308

Geisler D., Bica E., Dottori H., Clariá J. J., Piatti A. E., Santos J. F. C., Jr, 1997, AJ, 114, 1920

Geisler D., Piatti A. E., Bica E., Clariá J. J., 2003, MNRAS, 341, 771

Gilmore G., Wyse R. F.G., 1991, ApJ, 367, L55

Hodge P. W., Wright F. W., 1974, AJ, 79, 858

Kron G. E., 1956, PASP, 68, 125

Lauberts A., 1982, ESO/Uppsala Survey of the ESO (B) Atlas. European Southern Observatory, Munich

Lindsay E. M., 1958, MNRAS, 118, 172

Marconi G., Matteucci F., Tosi M., 1994, MNRAS, 270, 35

Olszewski E. W., Suntzeff N. B., Mateo M., 1996, ARA&A, 34, 511

Pagel B. E. J., Tautvaišienė G., 1998, MNRAS, 299, 535

Piatti A. E., Geisler D., Bica E., Clariá J. J., Santos J. F. C., Jr., Sarajedini A., Dottori H., 1999, AJ, 118, 2865

Piatti A. E., Santos J. F. C., Jr, Clariá J. J., Bica E., Sarajedini A., Geisler D., 2001, MNRAS, 325, 792

Piatti A. E., Sarajedini A., Geisler D., Bica E., Clariá J. J., 2002, MNRAS, 329, 556

Piatti A. E., Geisler D., Bica E., Clariá J. J., 2003a, MNRAS, 343, 851

Piatti A. E., Bica E., Geisler D., Clariá J. J., 2003b, MNRAS, 344, 965

Pietrzyński G., Udalski A., Kubiak M., Szymański M., Woźniak P., Zebruń K., 1998, Acta Astron., 48, 175

Rafelski M., Zaritsky D., 2005, AJ, in press (astro-ph/0408186)

Rich R. M., Shara M., Fall M., Zurek D., 2000, AJ, 119, 197

Schlegel D. J., Finkbeiner D. F., Davis M., 1998, ApJ, 500, 525

Stetson P. B., 1994, PASP, 106, 250

Stryker L. L., Da Costa G. S., Mould J. R., 1985, ApJ, 298, 544

This paper has been typeset from a TEX/LATEX file prepared by the author.